Liquid Crystals
Publication details, including instructions for authors and subscription information:
http://www.informaworld.com/smpp/title~content=t713926090

New temperature scan method (TSM) for revealing the chiral smectic polar phases

P. Simeão Carvalho[a]; M. Glogarová[ab]; M. R. Chaves[a]; C. Destrade[c]; Huu Tinh Nguyen[c]
[a] Departamento de Física, Faculdade de Ciĕncias da Universidade do Porto, Centro de Física da Universidade do Porto, Instituto Materiais (IMAT-Núcleo IFIMUP), Porto, Portugal [b] Institute of Physics, Academy of Sciences of the Czech Republic, Prague, Czech Republic [c] Centre de Recherche Paul Pascal, Pessac, France

To cite this Article Carvalho, P. Simeão , Glogarová, M. , Chaves, M. R. , Destrade, C. and Nguyen, Huu Tinh(1996) 'New temperature scan method (TSM) for revealing the chiral smectic polar phases', Liquid Crystals, 21: 1, 115 — 119

To link to this Article: DOI: 10.1080/02678299608033801

URL: http://dx.doi.org/10.1080/02678299608033801

LIQUID CRYSTALS, 1996, VOL. 21, NO. 1, 115–119

New temperature scan method (TSM) for revealing the chiral smectic polar phases

by P. SIMEÃO CARVALHO†, M. GLOGAROVÁ†‡, M. R. CHAVES†,
C. DESTRADE§ and HUU TINH NGUYEN§

†Departamento de Física, Faculdade de Ciências da Universidade do Porto,
Centro de Física da Universidade do Porto, Instituto Materiais (IMAT-Núcleo
IFIMUP), Rua do Campo Alegre, 687, 4150 Porto, Portugal
‡Institute of Physics, Academy of Sciences of the Czech Republic, Na Slovance 2,
180 40, Prague 8, Czech Republic
§Centre de Recherche Paul Pascal, Av. Schweitzer, 33600 Pessac, France

(*Received 17 November 1995; accepted 14 February 1996*)

A new simple and reliable method to identify the antiferro-, ferri- and ferro-electric and the $S^*_{C_\alpha}$ phases has been worked out, involving temperature scanning of the liquid crystalline sample under a square wave electric field. The d.c. current recorded during the temperature run provides information about the phases and the phase transition temperatures. The resolution power of the method is checked by the study of three compounds. The results obtained by this new Temperature Scan Method (TSM) are compared to those found from dielectric measurements and from the study of the optical and dielectric hysteresis loops.

1. Introduction

Since several liquid crystalline polar phases were discovered for the first time in MHPOBC [1], several compounds have been synthesized exhibiting such phases, namely ferroelectric, ferrielectric, and antiferroelectric phases and the $S^*_{C_\alpha}$ phase.

The identification of these phases is usually done by miscibility tests with a reference compound. The determination of their polar characteristics is achieved by conoscopic observations, by the study of dielectric and optical hysteresis loops and by measurements of the dielectric constant. It is often observed, however, that the use of each of these methods is not enough to disclose some polar phases, especially phases with similar polar properties or similar molecular arrangements. In those cases, the interpretation of conoscopic figures is ambiguous, hysteresis loops are not always conclusive and the dielectric constant may not show visible anomalies at the phase transitions.

In this paper we present a new Temperature Scan Method (TSM) which throws additional light on the properties of such polar phases. It is a powerful qualitative method to detect the polar phases known as the ferro-, ferri- and antiferro-electric phases and the $S^*_{C_\alpha}$ phase.

The study of three chiral compounds by this technique provided evidence for the simplicity and reliability of this new method. The phase sequences of these compounds, not clearly determined from studies of dielectric response, have been achieved by TSM. For one of the compounds, the phase assignment was checked by the study of optical hysteresis loops.

2. Description of the method

In this method, an a.c. electric field is applied to the liquid crystalline sample. The current flowing in the circuit is measured by an electrometer, as a voltage on a resistor R in series with the sample. Figure 1 shows the scheme of the electric circuit used.

When an electric field is applied to a liquid crystalline sample, the resulting current density flowing in the circuit is a sum of three contributions [2], J_i due to the dielectric constant (ε), J_P due to the polarization (P) and

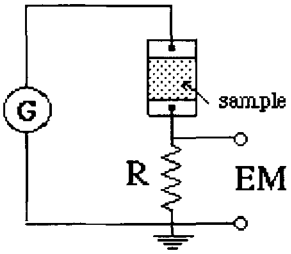

Figure 1. Electrical circuit used for the TSM. G is the function generator (HP33120A), EM is the electrometer (Keithley 617) and R is the resistor.

J_c due to the electric conductivity (σ):

$$J = \frac{\mathrm{d}(\varepsilon\mathbf{E})}{\mathrm{d}t} + \frac{\mathrm{d}P_s(t, T, \mathbf{E})}{\mathrm{d}t} + \sigma\mathbf{E}_l = J_i + J_P + J_c. \qquad (1)$$

P_s is the part of the spontaneous polarization which is reversed by the macroscopic electric field $\mathbf{E}$, and $\mathbf{E}_l$ is the local field, which is known to be a function of the switched polarization [3]. Assuming that ε is linear with the field and constant during one period of the a.c. applied field and that the temperature is changed at a constant rate ($\mathrm{d}T/\mathrm{d}t = \text{const.}$), we have:

$$J_i = \frac{\partial\varepsilon}{\partial T}\frac{\mathrm{d}T}{\mathrm{d}t}\mathbf{E} + \varepsilon\frac{\mathrm{d}\mathbf{E}}{\mathrm{d}t}$$

$$J_P = \frac{\partial P_s}{\partial t} + \frac{\partial P_s}{\partial T}\frac{\mathrm{d}T}{\mathrm{d}t} + \frac{\partial P_s}{\partial \mathbf{E}}\frac{\mathrm{d}\mathbf{E}}{\mathrm{d}t} = J_s + J_\lambda + J_E$$

$$J_c = \sigma\mathbf{E}_l.$$

The first term in J_i is sensitive to the temperature dependence of the dielectric constant and it can give an important contribution to $J(T)$ at the phase transition temperatures when ε changes sharply. The second term in J_i depends on ε and on the form of the applied electric field.

J_λ is the pyroelectric current density, which increases considerably in the vicinity of a phase transition, where the polarization changes significantly with temperature [4], e.g. at the $\mathrm{S}^*_{\mathrm{C_A}}$–$\mathrm{S}^*_{\mathrm{C}}$ and at the $\mathrm{S}^*_{\mathrm{C}}$–$\mathrm{S_A}$ phase transitions. It can be responsible for peaks in $J(T)$ at the transition temperatures.

J_s is produced by incomplete switching and therefore it is sensitive to the response of the polar phases. Its contribution to $J(T)$ depends on the macroscopic polarization imposed by the electric field (see figure 2). Figure 2 describes schematically the behaviour of the polarization for an increasing field, in ferro- (FE), ferri- (FI) and antiferro-electric (AFE) phases for a thick cell, where the helicoidal structure exists in the absence of the field.

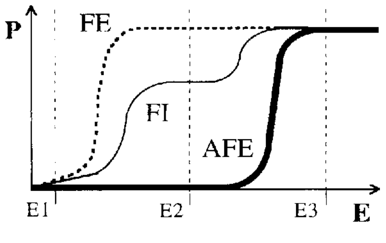

Figure 2. For a cell where a helicoidal structure exists in the absence of an electric field (E), the electric field dependence of the macroscopic polarization for increasing field is shown during quasi-static switching in the FE (dashed line), FI (thin line) and AFE (bold line) phases. The low (E1), high (E3) and intermediate (E2) fields are indicated by the dashed perpendiculars.

J_E depends on the form of the applied electric field. Its contribution can be more important when a sine or a triangular wave field is applied, but becomes negligible for a square wave. In this case, during the time when the field reversal occurs there is no polarization switching.

J_c is mostly of ionic origin in liquid crystals. It depends on the local field which is influenced by the polarization imposed by the macroscopic electric field. As is shown in figure 2, a low field (E1) produces a very low polarization in all ferro- (FE), ferri- (FI) and antiferro-electric (AFE) phases. A high field (E3) induces a saturated polarization in these phases and, as well as the low field, provides no relevant information about either the polar character or the transition temperatures of the different phases. Therefore, the choice of the electric field amplitude $\mathbf{E}$ is crucial in the experimental method here described. An intermediate 'proper' field (E2) must be chosen in order to disclose the polar character of the phases and their phase transition temperatures. Since the local field $\mathbf{E}_l$ depends on the switching polarization P_s, and being higher as P_s increases [3], then J_c will be sensitive to the polar characteristics of the phases.

The detected d.c. current is the average of the total current flowing through the resistor R in the positive and in the negative pulses, i.e.

$$\langle I\rangle = \left\langle \frac{\partial\varepsilon}{\partial T}\frac{\mathrm{d}T}{\mathrm{d}t}\mathbf{E} + \varepsilon\frac{\mathrm{d}\mathbf{E}}{\mathrm{d}t} + \frac{\partial P_s}{\partial t} + \frac{\partial P_s}{\partial T}\frac{\mathrm{d}T}{\mathrm{d}t} \right.$$
$$\left. + \frac{\partial P_s}{\partial\mathbf{E}}\frac{\mathrm{d}\mathbf{E}}{\mathrm{d}t} + \sigma\mathbf{E}_l \right\rangle S$$
$$= \langle J_i + J_s + J_\lambda + J_E + J_c\rangle S \qquad (2)$$

where S is the electrode area.

In the following, we assume that the temperature variation of the sample is negligible during a period of $\mathbf{E}(t)$. An immediate consequence of this assumption is that $\langle J_s\rangle = 0$, as well as the contribution from the $\varepsilon(\mathrm{d}\mathbf{E}/\mathrm{d}t)$ term, i.e. $\langle J_i\rangle = \langle(\partial\varepsilon/\partial T)(\mathrm{d}T/\mathrm{d}t)\mathbf{E}\rangle$. If the electric field has symmetrical values in two consecutive half periods, then $\langle I\rangle \approx \langle J_E\rangle S$; $\langle J_E\rangle$ is always negligible when a square wave field is applied to the sample. The contributions to $\langle I\rangle(T)$ coming from $\langle J_i + J_\lambda + J_c\rangle$ can only appear if some unbalanced response occurs, due to either external or internal factors. The level of $\langle I\rangle$ in each phase comes mostly from the contribution of J_c, while the peaks at the phase transitions come from J_i and J_λ.

Internal factors are defects or surface layers, which create an internal bias field. External factors, which are related to the applied electric field, are the offset and the duty factor of the square wave. The very low frequency might also be seen as another external factor, when there is a temperature change during the square wave period. This factor has not been considered in this study as a high enough frequency was used.

3. Experimental results

The three compounds used exhibit several polar phases, and two of them belong to the series

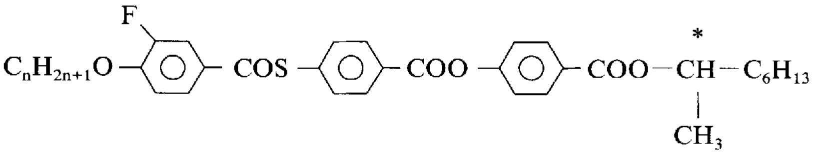

where $n = 9$ and 11 (9FHTBBM7 and 11FHTBBM7, respectively). The compound 9FHTBBM7 has the phase sequence [5]

$$\mathrm{Cr}\text{–}S^*_{C_A}\text{–}S^*_{C_{FI}}\text{–}S^*_C\text{–}S^*_{C_\alpha}\text{–}S_A\text{–}\mathrm{I}.$$

The 11FHTBBM7 displays the same sequence but without the $S^*_{C_\alpha}$ phase. The last compound is the mixture CS-4000, supplied by the Chisso Corporation, with the phase sequence

$$\mathrm{Cr}\text{–}S^*_{C_A}\text{–}S^*_C\text{–}S_A\text{–}\mathrm{I}.$$

This phase sequence has been provided by the Chisso Corporation.

The samples were filled into commercial cells from Linkam Scientific Instruments, ensuring planar anchoring, with the electrode spacing of 7·5 μm. All the measurements with the TSM were done on heating at a rate of 1·2 K min^{-1} with a 1 kHz square wave field and an offset lower than 1% of the field amplitude. Results of $\langle I\rangle(T)$ obtained with square, triangular and sine wave forms are similar, but the anomalies were more pronounced when using square waves.

3.1. *Results obtained with 9FHTBBM7 and 11FHTBBM7*

The d.c. current response $\langle I\rangle(T)$ detected by TSM on the compound 9FHTBBM7 is shown in figure 3(*a*) for applied electric fields of 0·4 and 0·7 V μm^{-1}. The low field curve shows an increase of the intensity $\langle I\rangle$ around 97°C, which can be identified with the onset of the S^*_C phase. In the upper temperature range of this phase a slight variation of the intensity is observed. The slight decrease of $\langle I\rangle(T)$ at 105°C and the subsequent decrease at ≈107°C define the limits of the temperature range of the $S^*_{C_\alpha}$ phase.

The high field curve exhibits an additional clear peak around 86°C not observed in the low field curve and discloses the $S^*_{C_A}$–$S^*_{C_{FI}}$ phase transition. The peak at ≈107°C corresponds to the $S^*_{C_\alpha}$–S_A transition which is more pronounced under the higher field. The $S^*_{C_\alpha}$ phase is located between this peak and the minimum of $\langle I\rangle(T)$ at ≈105°C.

The relevance of the TSM can be seen by comparing the results obtained by this technique with those found from the temperature dependence of the dielectric constant measured at a frequency of 20 Hz (see figure 3(*b*),

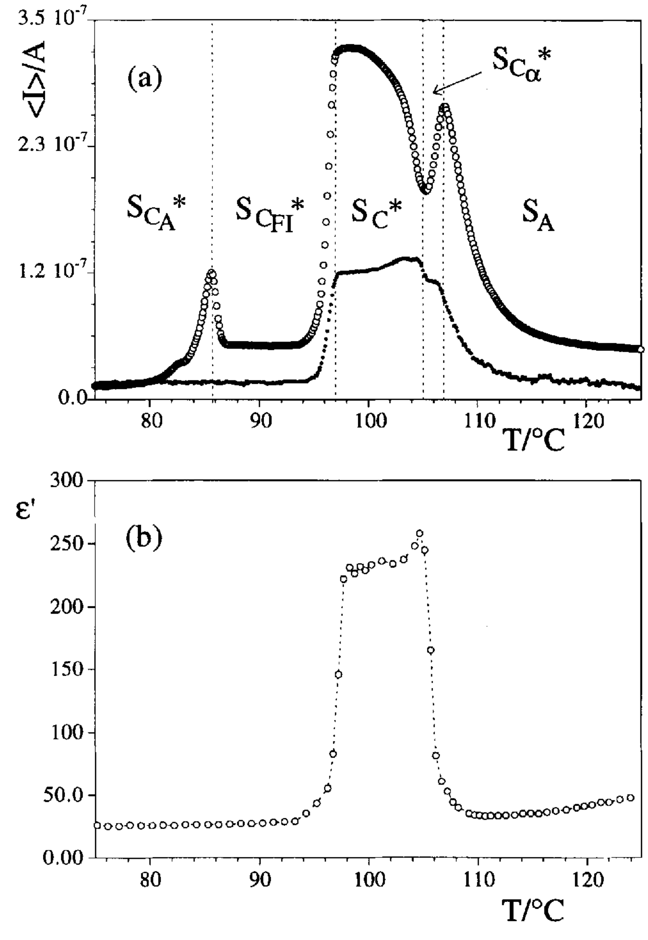

Figure 3. (*a*) $\langle I\rangle$ recorded during the temperature scan for 9FHTBBM7 under fields of 0·4 V μm^{-1} (full circles) and 0·7 V μm^{-1} (open circles); (*b*) temperature dependence of the dielectric constant for 9FHTBBM7, measured on a heating run at a frequency of 20 Hz.

taken from ref. [5]). The high values in ε' between 97°C and 105°C have been identified with the range of the S_C^* phase, but with dielectric measurements it was not possible to determine from figure 3 (*b*) either the temperature range of the $S_{C_\alpha}^*$ phase, or the $S_{C_A}^*$–$S_{C_{FI}}^*$ transition temperature. The temperature scan method gives here the complete phase sequence in contrast to the study of $\varepsilon(T)$. One must however point out that for some other compounds, both the $S_{C_\alpha}^*$ phase and the $S_{C_A}^*$–$S_{C_{FI}}^*$ phase transition could be seen by dielectric measurements [6].

The phase sequence found by TSM has been confirmed by observation of optical hysteresis loops (see figure 4), which reflect characteristic features of the assigned phases [5, 7].

For the compound 11FHTBBM7, we present the current $\langle I \rangle$ as a function of the temperature in figure 5. The electric field amplitude chosen (0·3 V μm^{-1}) allows detection of the full phase sequence. The peak around 73°C is related to the $S_{C_A}^*$–$S_{C_{FI}}^*$ phase transition, the subsequent increase of $\langle I \rangle$ at 94°C corresponds to the $S_{C_{FI}}^*$–S_C^* phase transition and the decrease at 115°C to

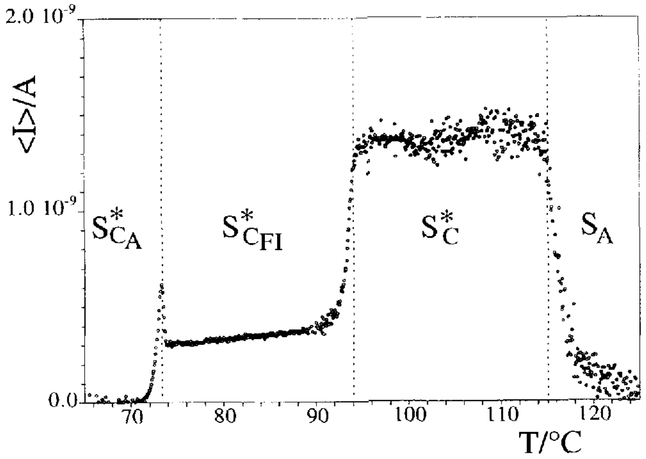

Figure 5. $\langle I \rangle$ recorded during the temperature scan for 11FHTBBM7 under a field of 0·3 V μm^{-1}.

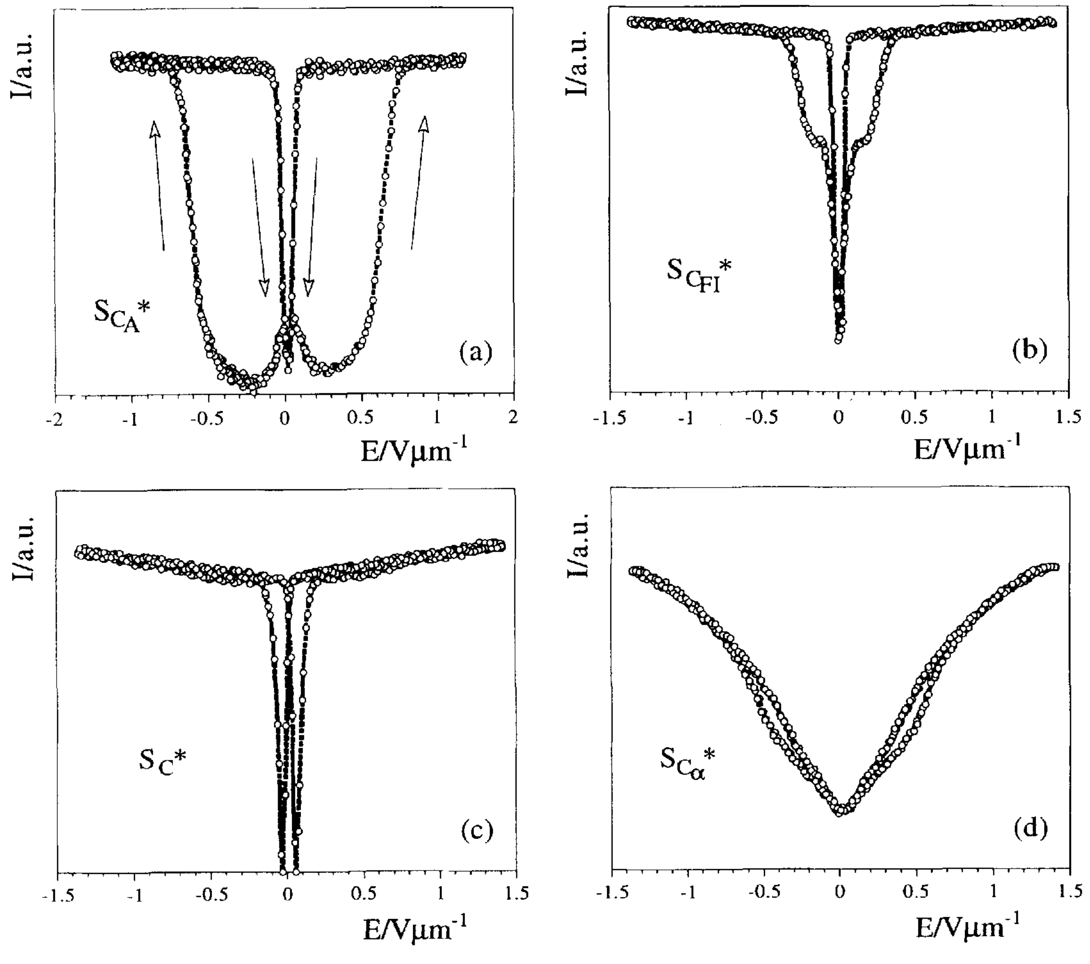

Figure 4. Optical hysteresis loops for 9FHTBBM7 at (*a*) 72°C ($S_{C_A}^*$), (*b*) 88°C ($S_{C_{FI}}^*$), (*c*) 98°C (S_C^*) and (*d*) 107°C ($S_{C_\alpha}^*$).

the transition to the S_A phase. $\langle I\rangle(T)$ has the highest value in the ferroelectric S_C^* phase, is lower in the ferrielectric $S_{C_{FI}}^*$ phase and is very low in the antiferroelectric $S_{C_A}^*$ and paraelectric S_A phases. In all these phases, the major contribution to $\langle I\rangle(T)$ comes from J_c as referred to previously. The peak at 73°C can be due either to J_i or J_λ, or both.

The phase sequence detected by TSM has been confirmed by observation of dielectric hysteresis loops.

3.2. *Results obtained with the mixture CS-4000*

According to Chisso Corporation data, CS-4000 exhibits the antiferroelectric $S_{C_A}^*$, the ferroelectric S_C^* and the paraelectric S_A phases between -10°C and 100°C. Figure 6 depicts two curves obtained from TSM, for applied electric field amplitudes of $0{\cdot}4\,\mathrm{V\,\mu m^{-1}}$ and $1\,\mathrm{V\,\mu m^{-1}}$. On the low field curve, the S_C^* phase limits are given by the steep increase and decrease of $\langle I\rangle$ around 82°C and 84°C, respectively. In the $S_{C_A}^*$ and S_A phases, $\langle I\rangle$ is very small. This behaviour is expected in the antiferro- and in the para-electric phases under a low field.

At ≈ 80°C, a kink can be observed on the low field curve. For the high field curve, this kink is still seen at the same temperature and seems to be related to a transition to another polar phase, not reported in the Chisso Corporation data. At high field, the maximum at 82°C can no longer be observed, while the maximum at ≈ 84°C becomes more pronounced.

Recently, DSC studies [8] on this compound revealed anomalies which were related to the existence of a ferrielectric phase (between the $S_{C_A}^*$ and the S_C^* phases) and to the $S_{C_\alpha}^*$ phase (between the S_C^* and the S_A phases). The TSM results clearly detect the existence of the ferrielectric phase as can be seen in the low field curve of figure 6. The higher electric field provides evidence for the transition from the antiferroelectric phase to the ferrielectric phase, but seems to be too high to identify the ferrielectric–ferroelectric phase transition. The upper limit of the S_C^* is clearly observed in both curves. However no evidence was found by TSM for the $S_{C_\alpha}^*$ phase or for the $S_{C_\alpha}^*$–S_A phase transition, probably because of the weak polar character of the $S_{C_\alpha}^*$ phase in this material.

4. Conclusion

The present study has provided clear evidence for the relevance of the Temperature Scan Method to the study of compounds with polar mesophases. It is a simple and reliable method which, when used in an appropriate manner, can reveal the different polar phases in chiral smectics. The TSM is particularly useful for disclosing the $S_{C_{FI}}^*$ phase and, in some cases, the $S_{C_\alpha}^*$ phase, when they cannot be easily identified from the study of the temperature dependence of the dielectric constant.

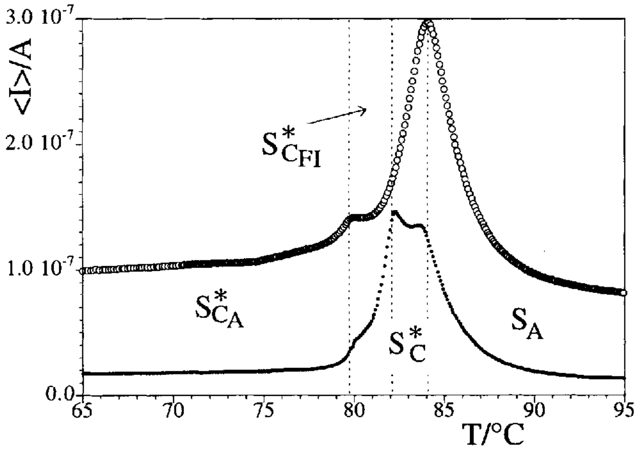

Figure 6. $\langle I\rangle$ recorded during the temperature scan for CS-4000 under fields of $0{\cdot}4\,\mathrm{V\,\mu m^{-1}}$ (full circles) and $1\,\mathrm{V\,\mu m^{-1}}$ (open circles).

The authors are deeply indebted to Albano Costa for technical assistance and to Dr J.-P. Marcerou for stimulating discussions. This work was partially supported by JNICT and by 'Service Culturel Scientifique et de Coopération de l'Ambassade de France au Portugal'. One of us (M.G.) is grateful to JNICT for the grant PRAXIS XXI/BCC/4377/94.

References

[1] Chandani, A. D. L., Gorecka, E., Ouchi, Y., Takezoe, H., and Fukuda, A., 1989, *Jpn. J. appl. Phys.*, **28**, L1256.
[2] Martinot-Lagard, P., 1988, *Ferroelectrics*, **84**, 53.
[3] Kittel, C., 1976, *Solid State Physics* (New York: J. Wiley & Sons Inc.).
[4] Lines, M. E., and Glass, A. M., 1977, *Principles and Applications of Ferroelectrics and Related Materials* (Oxford: Clarendon Press).
[5] Simeão Carvalho, P., Chaves, M. R., Destrade, C., Nguyen, H. T., and Glogarová, M., *Liq. Cryst.* (in the press).
[6] Hiraoka, K., Tagushi, A., Ouchi, Y., Takezoe, H., and Fukuda, A., 1990, *Jpn. J. appl. Phys.*, **29**, L103.
[7] Orihara, H., Fujikawa, T., Ishibashi, Y., Yamada, Y., Yamamoto, K., Mori, K., Nakamura, K., Suzuki, Y., Hagiwara, T., and Kawamura, I., 1990, *Jpn. J. appl. Phys.*, **23**, L333.
[8] Le Bourhis, L., Dupont, L., and Destrade, C., *Ferroelectrics* (to be published).